Localisation and identification of sources on laminated structures: extension of CFAT method

Fabien Marchetti, Kerem Ege, Quentin Leclere

NOVEM 2018
Noise and vibration emerging methods
The 6th conference, 7 – 9 May 2018
Ibiza – Spain

LOCALISATION AND IDENTIFICATION OF SOURCES ON LAMINATED STRUCTURES : EXTENSION OF CFAT METHOD

F. Marchetti[1*] , K. Ege[1] and Q. Leclère[1]

[*]Email: fabien.marchetti@insa-lyon.fr

[1] Laboratoire Vibrations Acoustique de l'INSA de Lyon,
25 bis, avenue Jean Capelle, 69621 VILLEURBANNE Cedex, FRANCE

ABSTRACT

In the literature, several papers deal with the localisation and quantification of forces on a structure. One of them, the FAT (Force Analysis Technique) method, which was recently extended to material characterisation, was initially created for vibration source identification. This method was developed for beams, isotropic plates or shells and recently orthotropic plates. FAT identifies the equation of motion of the structure with a finite difference scheme applied on a measured displacement field. This scheme gives an approximation of the partial derivatives. By introducing correction factors, the CFAT (Corrected FAT) methodology corrects the approximation made by finite difference scheme and attenuates the singularities of the filter. This paper presents the extension of this last method for laminated plates. This type of plate is different from an orthotopic plate because it presents a flexural-torsion interaction and has a complex equation of motion with 5 flexural rigidities (against 3 in the orthotropic case and 1 in the isotropic case). The correction of the finite difference scheme is now composed of 5 correction factors estimated in this paper analytically and numerically. Finally, a validation of the extension of CFAT is presented on numerical displacement field (FEM Nastran) for laminated plates.

1 INTRODUCTION

Localising and quantifying sources for vibro-acoustical applications is a major issue for the community. The accurate identification of exitations is essential to understand the behaviour of the system especially for complex structures. Several studies have been published on the quantification topic, based on direct and inverse problems in multiple degree of freedom systems [1].

The Force Analysis Technique (FAT) is an alternative experimental method which uses the displacement field of a local part of the structure to localize and quantify the sources. The local aspect allows to use the method without any knowledge outside the studied area (boundary conditions, other sources, other dynamical properties). FAT has been developed for beams [2], plates [3] and shells [4] and is based on the use of the equation of motion that describes the equilibrium of internal and external forces applied on the structure. A finite difference scheme applied on the measurement mesh gives an approximation of the partial derivatives of the equation of motion.

In practice, this approximation is very sensitive to measurement uncertainties. That's why several techniques have been adopted like the use of a low-pass wavenumber filtering [2] [3] or the use of adapted spacings [5]. Another approach, called CFAT (Corrected FAT) [6], corrects the bias error of the finite difference scheme.

These methodologies can also be used for the identification of the structural parameter by studing the measurement area far away from the source and neglecting the applied forces in the equation of motion. Material characteristics of beams and isotropic plates have been estimated using FAT in [7] CFAT in [8]. Recently, FAT has been adapted to deal with orthotropic structures [9].

This paper presents the extension of CFAT method for the identification of sources on laminated (composite) plates. This type of structures, constituted from several orthotropic layers with different orientation angle, present a more complex equation of motion and the corrected finite difference scheme must be adapted. In a first part, the methodology of calculation of the correction is presented for the laminated case analytically and numerically. And, in a second part, numerical applications are shown on the identification of sources.

2 METHODOLOGY

2.1 Definitions

The FAT is applied on the displacement field $w(x, y)$ of a plate, measured with a rectangular mesh. The mesh is chosen in order to respect Shannon's spatial criterion. The spacing between two consecutive points in the x and y axes are given by:

$$d_x < \frac{\lambda_{\mathrm{N},x}(f_{\max})}{2} \quad ; \quad d_y < \frac{\lambda_{\mathrm{N},y}(f_{\max})}{2} \tag{1}$$

where $\lambda_{\mathrm{N},x}$ and $\lambda_{\mathrm{N},y}$ represent respectively the natural wavelength of the plate in the x and y axis and $f_{\max}$ the upper bound of the frequency bandwidth of interest.

The FAT theory is based on the equation of motion of Love-Kirchhoff thin plate theory. For a laminated plate, for which flexural-torsion interactions exist, it is written as follows:

$$D_{11}\frac{\partial^4 w}{\partial x^4} + D_{22}\frac{\partial^4 w}{\partial y^4} + D_{12}\frac{\partial^4 w}{\partial x^2 \partial y^2} + D_{16}\frac{\partial^4 w}{\partial x^3 \partial y} + D_{26}\frac{\partial^4 w}{\partial x \partial y^3} - \rho h \omega^2 w(x, y) = p(x, y) \tag{2}$$

where the coefficients D_{ij}, p and ω represent respectively the flexural rigidities, the pressure field exciting the plate and the angular frequency. Contrarily to orthotropic structures for which only 3 flexural rigidities are needed (D_{11}, D_{22}, D_{12}), the rigidities D_{16}, D_{26} are not null for laminated plates due to the flexural-torsion interaction.

FAT method estimates the pressure field by identifying the partial derivatives of the equation of motion (2) with a finite difference scheme applied to the displacement field [9]:

$$\frac{\partial^4 w}{\partial x^4} \approx \delta^{4x} = \frac{1}{16\Delta_x^4}\left(w_{i+4,j} - 4w_{i+2,j} + 6w_{i,j} - 4w_{i-2,j} + w_{i-4,j}\right) \tag{3}$$

$$\frac{\partial^4 w}{\partial y^4} \approx \delta^{4y} = \frac{1}{16\Delta_y^4}\left(w_{i,j+4} - 4w_{i,j+2} + 6w_{i,j} - 4w_{i,j-2} + w_{i,j-4}\right) \tag{4}$$

$$\begin{aligned}\frac{\partial^4 w}{\partial x^2 \partial y^2} \approx \delta^{2x2y} = \frac{1}{16\Delta_x^2\Delta_y^2}\big(&w_{i+2,j+2} + w_{i+2,j-2} + w_{i-2,j+2} + w_{i-2,j-2} \\ &-2(w_{i+2,j} + w_{i-2,j} + w_{i,j+2} + w_{i,j-2}) + 4w_{i,j}\big)\end{aligned} \tag{5}$$

$$\begin{aligned}\frac{\partial^4 w}{\partial x^3 \partial y} \approx \delta^{3xy} = \frac{1}{16\Delta_x^3\Delta_y}\big(&w_{i+3,j+1} - w_{i+3,j-1} - w_{i-3,j+1} + w_{i-3,j-1} \\ &-3(w_{i+1,j+1} - w_{i+1,j-1} - w_{i-1,j+1} + w_{i-1,j-1})\big)\end{aligned} \tag{6}$$

$$\begin{aligned}\frac{\partial^4 w}{\partial x \partial y^3} \approx \delta^{x3y} = \frac{1}{16\Delta_x\Delta_y^3}\big(&w_{i+1,j+3} - w_{i-1,j+3} - w_{i+1,j-3} + w_{i-1,j-3} \\ &-3(w_{i+1,j+1} - w_{i+1,j-1} - w_{i-1,j+1} + w_{i-1,j-1})\big)\end{aligned} \tag{7}$$

The finite difference scheme is finally composed of 25 points. Δ_x and Δ_y represent the half of the spacing between two consecutive points of the scheme in the x and y axes (see Figure 1). In order to reduce the amplification of noise and the estimation error, the scheme size must be adapted as a function of the frequency. Natural integers (p_x, p_y) are introduced at each frequency f so that the number of points per wavelength (n_x, n_y) respects the conditions:

$$2 < n_x = \frac{\lambda_{\mathrm{N},x}(f)}{2p_x d_x} < 4 \quad ; \quad 2 < n_y = \frac{\lambda_{\mathrm{N},y}(f)}{2p_y d_y} < 4 \tag{8}$$

This condition is adapted from [5] where it was established for the isotropic case. In practice, the optimal value of (p_x, p_y) is reached when n_x, n_y are the nearest of the value of 3. The impact of the evolution of n_x and n_y on FAT and CFAT will be shown in the third part.

Then, Δ_x and Δ_y can be linked to the mesh by : $\Delta_x = p_x d_x$ and $\Delta_y = p_y d_y$. Figure 1 gives an example of two schemes (one with $p_x = p_y = 1$ and the other with $p_x = 2$ and $p_y = 1$):

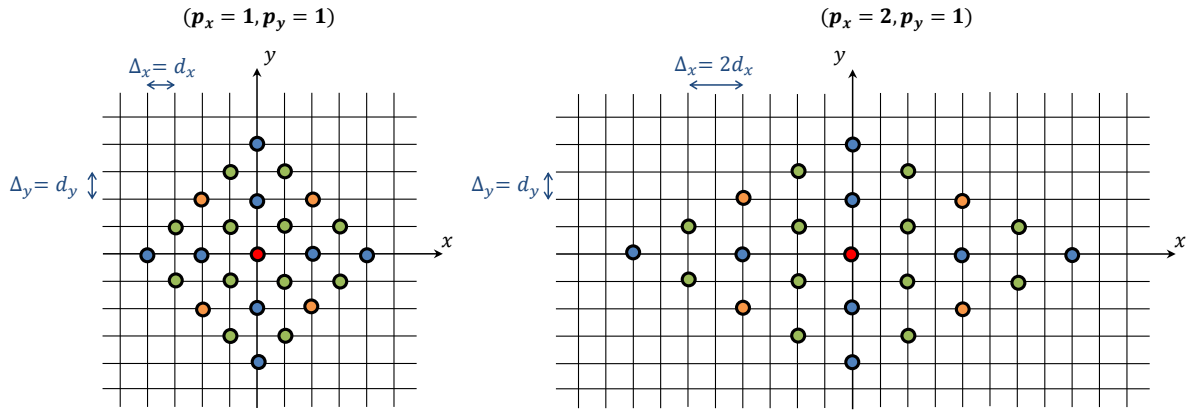

Figure 1. Example of finite difference schemes adapted for two frequencies.

The red dot ● corresponds to $w_{i,j}$. Blue dots ● correspond to the terms of δ^{4x} and δ^{4y}. Orange dots ● correspond to the terms of δ^{2x2y}. Green dots ● correspond to the terms of δ^{3xy} and δ^{x3y}. Finally, the FAT estimation of the pressure field is:

$$D_{11}\delta^{4x} + D_{22}\delta^{4y} + D_{12}\delta^{2x2y} + D_{16}\delta^{3xy} + D_{26}\delta^{x3y} - \rho h\omega^2 w(x,y) = p^{\text{fat}}(x,y) \tag{9}$$

This estimation is biased by an error caused by the finite differences approximation. This bias error can be strongly attenuated by introducing correction factors (CFAT method). Those correction factors, μ_{ij}, multiplying each δ^{ij}, transform the Eq. (9) to:

$$\begin{aligned} D_{11}\mu_{11}\delta^{4x} + D_{22}\mu_{22}\delta^{4y} + D_{12}\mu_{12}\delta^{2x2y} + D_{16}\mu_{16}\delta^{3xy} \\ + D_{26}\mu_{26}\delta^{x3y} - \rho h\omega^2 w(x,y) = p^{\text{cfat}}(x,y) \end{aligned} \tag{10}$$

The μ_{ij} are identified by analysing the error between the Eq. (2) and (10) in the wavenumber domain.
The Fourier transform of Eq. (2) is:

$$\left(D_{11}k_x^4 + D_{22}k_y^4 + D_{12}k_x^2k_y^2 + D_{16}k_x^3k_y + D_{26}k_xk_y^3 - \rho h\omega^2\right)\widehat{w}(k_x,k_y) = \widehat{p}(k_x,k_y) \tag{11}$$

with $\widehat{p}$ and $\widehat{w}$ the Fourier transforms of p and w.
The Fourier transform of the finite difference scheme is:

$$\widehat{\delta}^{4x} = \frac{\widehat{w}(k_x,k_y)}{\Delta_x^4}\sin^4(k_x\Delta_x) \tag{12}$$

$$\widehat{\delta}^{4y} = \frac{\widehat{w}(k_x,k_y)}{\Delta_y^4}\sin^4(k_y\Delta_y) \tag{13}$$

$$\widehat{\delta}^{2x2y} = \frac{\widehat{w}(k_x,k_y)}{\Delta_x^2\Delta_y^2}\sin^2(k_x\Delta_x)\sin^2(k_y\Delta_y) \tag{14}$$

$$\widehat{\delta}^{3xy} = \frac{\widehat{w}(k_x,k_y)}{\Delta_x^3\Delta_y}\sin^3(k_x\Delta_x)\sin(k_y\Delta_y) \tag{15}$$

$$\widehat{\delta}^{x3y} = \frac{\widehat{w}(k_x,k_y)}{\Delta_x\Delta_y^3}\sin(k_x\Delta_x)\sin^3(k_y\Delta_y) \tag{16}$$

Therefore, the spatial Fourier transform of the pressure field estimated by CFAT is:

$$\begin{aligned} \left(\frac{D_{11}\mu_{11}X^4}{\Delta_x^4} + \frac{D_{22}\mu_{22}Y^4}{\Delta_y^4} + \frac{D_{12}\mu_{12}X^2Y^2}{\Delta_x^2\Delta_y^2} + \frac{D_{16}\mu_{16}X^3Y}{\Delta_x^3\Delta_y}\right. \\ \left. + \frac{D_{26}\mu_{26}XY^3}{\Delta_x\Delta_y^3} - \rho h\omega^2\right)\widehat{w}(k_x,k_y) = \widehat{p}^{\text{cfat}}(k_x,k_y) \end{aligned} \tag{17}$$

with $X = \sin(k_x\Delta_x)$ and $Y = \sin(k_y\Delta_y)$.
The error of CFAT is the ratio between identified load and real distributions in the wavenumber domain:

$$E(\omega,\Delta_x,\Delta_y,k_x,k_y) = \frac{\widehat{p}^{\text{cfat}}(k_x,k_y)}{\widehat{p}(k_x,k_y)} \tag{18}$$

For reasons of simplicity, all calculations are now made in a polar reference system (k,θ) with $k_x = k\cos(\theta)$ and $k_y = k\sin(\theta)$. The roots of the dispersion relation Eq. (19) define the natural (flexural) wavenumbers k_N of the plate:

$$k^4\left[D_{11}c^4 + D_{22}s^4 + D_{12}c^2s^2 + D_{16}c^3s + D_{26}cs^3\right] = \rho h\omega^2, \tag{19}$$

with $c = \cos(\theta)$ and $s = \sin(\theta)$.
That's why, the ratio (18) presents a singularity when k is located at the natural wavenumber ($k = k_{\mathrm{N}}$) of the plate. This singularity is deleted by finding values of the correction factors that allow to have:

$$\widehat{p}^{\mathrm{cfat}}(k_{\mathrm{N}}, \theta) = 0 \tag{20}$$

This equation can be resolved by an analytical or numerical way.

2.2 Analytical correction factors

The 5 correction factors can be identified by resolving Eq. (20) with 5 different angles θ. Figure 2 gives an example of the imposed values shown on the k-space representation of the natural wavenumber of a laminated plate (studied in part 2.4):

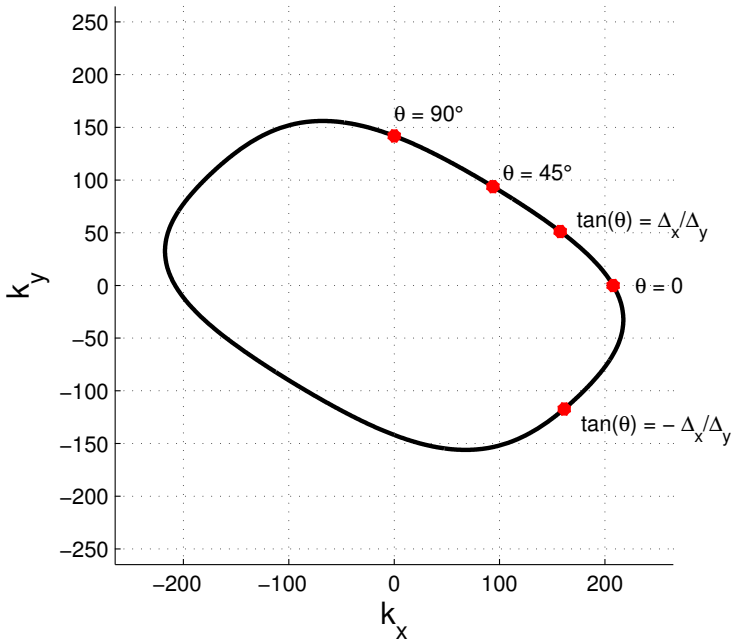

Figure 2: Representation of the imposed values used in the analytical calculation of the correction factors.

The first imposed value is $\theta = 0$ (that means $k_{\mathrm{N}} = \sqrt[4]{\frac{\rho h \omega^2}{D_{11}}}$ with Eq. (19)). Then, Eq. (20) becomes:

$$D_{11}\mu_{11}\sin^4(k_{\mathrm{N}}\Delta_x) = \rho h \omega^2 \Delta_x^4 \tag{21}$$

From the definition of the number of points per natural wavelength n_x in Eq. (8), the expression of the first correction factor is :

$$\mu_{11} = \frac{1}{\mathrm{sinc}^4(\frac{\pi}{n_x})} \tag{22}$$

The same process can also be done for the second correction factor with the imposed value $\theta = 90°$ (and $k_{\mathrm{N}} = \sqrt[4]{\frac{\rho h \omega^2}{D_{22}}}$):

$$\mu_{22} = \frac{1}{\mathrm{sinc}^4(\frac{\pi}{n_y})} \tag{23}$$

The solution of the other correction factors are more complex than the two first ones. Their detailed calculation (based on the use the three other imposed values of θ, see Figure 2) won't be

presented in this paper and only their expression is shown:

$$\mu_{12} = \frac{\Delta_x^2 \Delta_y^2}{D_{12}} \left[\frac{\rho h \omega^2}{2} \left(\frac{1}{\sin^4\left(\sqrt[4]{\frac{\rho h \omega^2}{A_1}}\right)} + \frac{1}{\sin^4\left(\sqrt[4]{\frac{\rho h \omega^2}{A_2}}\right)} \right) - \frac{D_{11}\mu_{11}}{\Delta_x^4} - \frac{D_{22}\mu_{22}}{\Delta_y^4} \right] \tag{24}$$

$$\mu_{16} = \frac{\Delta_x^3 \Delta_y}{D_{16}} \left[\frac{\rho h \omega^2 - \frac{D_{11}\mu_{11}}{\Delta_x^4} A_4^4 - \frac{D_{22}\mu_{22}}{\Delta_y^4} A_5^4 - \frac{D_{12}\mu_{12}}{\Delta_x^2 \Delta_y^2} A_4^2 A_5^2 - A_3 A_4 A_5^3}{(A_4^3 A_5 - A_4 A_5^3)} \right] \tag{25}$$

$$\mu_{26} = \frac{\Delta_x \Delta_y^3}{D_{26}} \left[A_3 - \frac{D_{16}^* \mu_{16}}{\Delta_x^3 \Delta_y} \right] \tag{26}$$

with:

$$\begin{aligned}
A_1 &= \tfrac{D_{11}}{\Delta_x^4} + \tfrac{D_{22}}{\Delta_y^4} + \tfrac{D_{12}}{\Delta_x^2 \Delta_y^2} + \tfrac{D_{16}}{\Delta_x^3 \Delta_y} + \tfrac{D_{26}}{\Delta_x \Delta_y^3} \\
A_2 &= \tfrac{D_{11}}{\Delta_x^4} + \tfrac{D_{22}}{\Delta_y^4} + \tfrac{D_{12}}{\Delta_x^2 \Delta_y^2} - \tfrac{D_{16}}{\Delta_x^3 \Delta_y} - \tfrac{D_{26}}{\Delta_x \Delta_y^3} \\
A_3 &= \tfrac{\rho h \omega^2}{2} \left(\frac{1}{\sin^4\left(\sqrt[4]{\frac{\rho h \omega^2}{A_1}}\right)} - \frac{1}{\sin^4\left(\sqrt[4]{\frac{\rho h \omega^2}{A_2}}\right)} \right) \\
A_4 &= \sin\left(\sqrt[4]{\tfrac{\rho h \omega^2}{D_{11}+D_{22}+D_{12}+D_{16}+D_{26}}} \Delta_x \right) \\
A_5 &= \sin\left(\sqrt[4]{\tfrac{\rho h \omega^2}{D_{11}+D_{22}+D_{12}+D_{16}+D_{26}}} \Delta_y \right)
\end{aligned}$$

2.3 Numerical correction factors

The correction factors can also be identified by resolving Eq. (20) with a multitude of values of angle θ from 0 to π (k_n is π periodic). k_N is identified with the dispersion relation Eq. (19).Finally, we obtain a system of equations where only the correction factors μ_{ij} are unknown:

$$[B]\{\mu_{ij}\} = [C] \tag{27}$$

with:

$$[B] = \begin{bmatrix} D_{11}^* X_i^4 & D_{22}^* Y_i^4 & D_{12}^* X_i^2 Y_i^2 & D_{16}^* X_i^3 Y_i & D_{26}^* X_i Y_i^3 \\ \vdots & \vdots & \vdots & \vdots & \vdots \end{bmatrix}$$

$$[C] = \begin{bmatrix} \rho h \omega^2 \\ \vdots \end{bmatrix}$$

where $X_i = \sin\left(k_\mathrm{N}(\theta_i)\cos(\theta_i)\Delta_x\right)$ and $Y_i = \sin\left(k_\mathrm{N}(\theta_i)\sin(\theta_i)\Delta_y\right)$.

This system can be resolved with a least square method:

$$\{\mu_{ij}\} = \frac{[B]^\mathrm{H}[C]}{[B]^\mathrm{H}[B]} \tag{28}$$

This numerical resolution depends on the number of equations used to create matrix $[B]$ and $[C]$. Different examples of the influence of this number on the wavenumber response of CFAT presented on section 2.1 are shown in the next section.

2.4 Comparison between numerical and analytical correction factors

Different comparisons between FAT and CFAT with analytical and numerical correction factors have been realised on two example of composite plates. Both plates are composed of 4 identical (carbon) layers. The first is orthotropic with layers oriented at $0°/0°/0°/0°$ and the second is a laminated plate with layers oriented at $60°/-60°/-60°/60°$. The characteristics of one layer are presented in the Table 1. The equivalent flexural rigidities of each plates were finally calculated with an equivalent single layer model [10].

h (m)	ρ (kg.m^{-3})	E_x (GPa)	E_y (GPa)	G_{xy} (GPa)	ν_{xy} (-)
0.187	1540	138	9.5	3.4	0.3

Table 1: Characteristics of one (carbon) layer of the studied orthotropic and laminated multilayer plates.

We represent the wavenumber responses (Eq. (18)) for the orthotropic and laminated plates as a function of k_x and k_y arbitrarily normalized by k_{av}, the average of $k_N(\theta)$. The correction is here presented for the standard value of number of points per wavelength ($n_x = n_y = 3$) although in practice they are not exactly equal to this value. Numerical correction factors were calculated with 50 equations using the least squares method. Figure 3 and 4 present the results of the three methods :

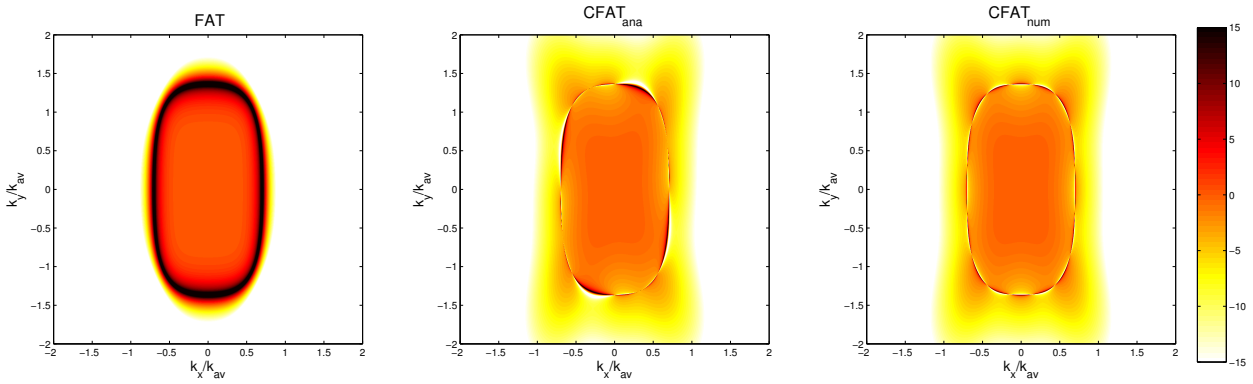

Figure 3: Wavenumber responses (dB) of FAT and CFAT with analytical and numerical (50 equations) correction factors for the orthotropic case with $n_x = n_y = 3$.

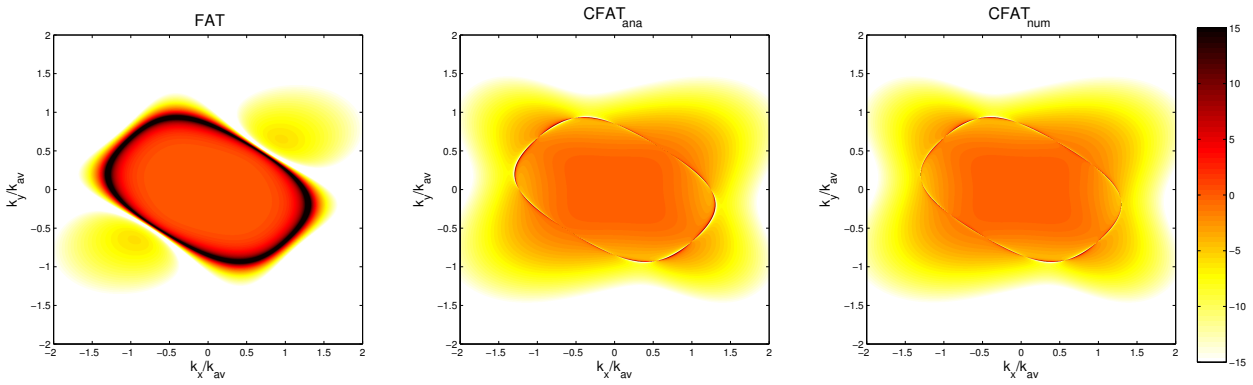

Figure 4: Wavenumber responses (dB) of FAT and CFAT with analytical and numerical (50 equations) correction factors for the laminated case with $n_x = n_y = 3$.

The singularity is clearly observed on FAT responses when $k = k_{\mathrm{N}}$. The correction of CFAT attenuates this singularity both for analytical and numerical strategies. The singularity disappears for some points. For the analytical case, these points are defined by the imposed values of $(k_{\mathrm{N},x}, k_{\mathrm{N},y})$. Other imposed values will change the angular position of these points. For the numerical case, the cancellation of the singularity depends on the number of equations used in the least squares estimation.

Figure 5 presents an example of wavenumber responses for different number of equations for the laminated case:

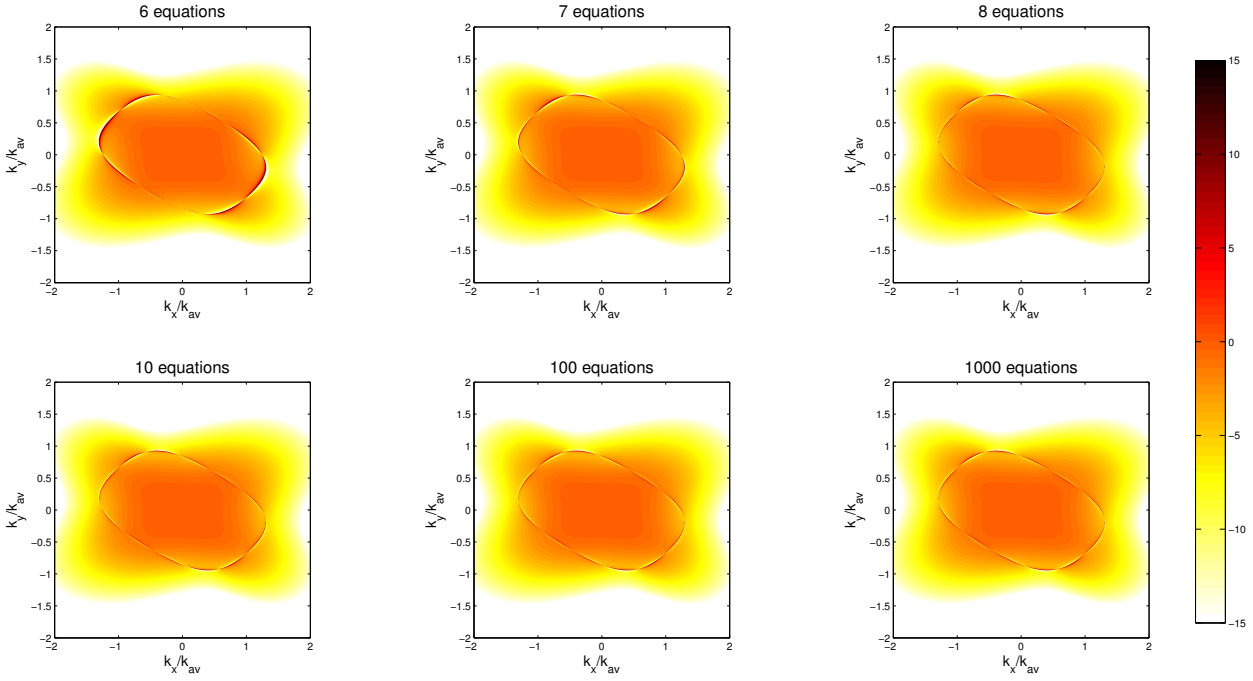

Figure 5: Wavenumber responses (dB) of $\mathrm{CFAT}_{\mathrm{num}}$ in function of number of equations used in the determination of the numerical correction factors in the laminated case with $n_x = n_y = 3$.

From a given number of equations, the wavenumber response remains practically unchanged showing more cancellation points than the analytical case. Indeed, least square method searches for values of correction factors that minimise the singularity. When the number of equations increases, correction factors converge to some asymptotic values. Finally, the numerical method has the advantage of being easier to implement with a better distribution of the attenuation of the singularity than the analytical method.

Figure 6 presents the evolution of the wavenumber response of CFAT with numerical correction factors (50 equations) for the laminated plate in function of the number of points per wavelength. We imposed $n_x = n_y$ varying from the limits of the condition (8): from 2 to 4.

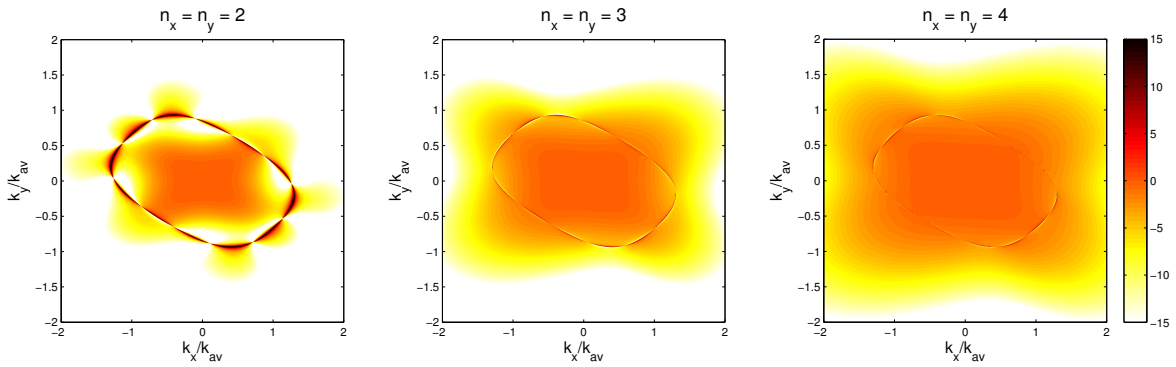

Figure 6: Wavenumber responses (dB) of CFAT_{num} (50 equations) in function of number of points per wavelength in the laminated case.

Without noise, increasing the number of points improves the attenuation of the singularity: a high number of points is an optimal choice. In real condition, with noise, a high number of points increase artificially the level of noise and scrambles the identification of the source as it is shown in the third part. For such real case, the optimal choice consists to tend to the value of 3 (see [5] for more details).

3 NUMERICAL APPLICATIONS FOR THE IDENTIFICATION OF SOURCES

The extension of CFAT method was applied on numerical displacement fields generated using the finite element software Nastran for the same plates as presented in the previous section. The shape of the plates is a square of 1 meter sideways, entirely meshed with a 400x400 points mesh. The boundary conditions are simply supported. The type of analysis applied on Nastran is a frequency response (Sol 111). The finite difference scheme is adapted in function of the frequency as it is written in the first part (see Eq. (8)). The applied force, of a value of 1 N, is located at the same place for the two plates ($x = 0,335$ m, $y = 0,695$ m). Figure 7 and 8 present a comparison between the pressure field estimated by FAT and CFAT methods with the numerical correction factors. The results are shown at $f = 5000$ Hz for the two plates:

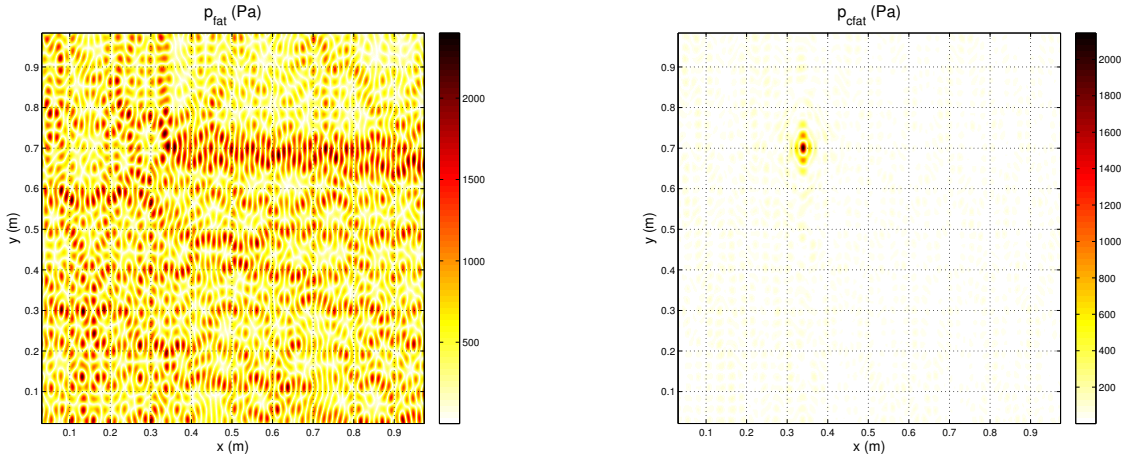

Figure 7: Pressure field estimated with FAT and CFAT_{num} (50 equations) on the orthotropic structure with $n_x = n_y = 3$.

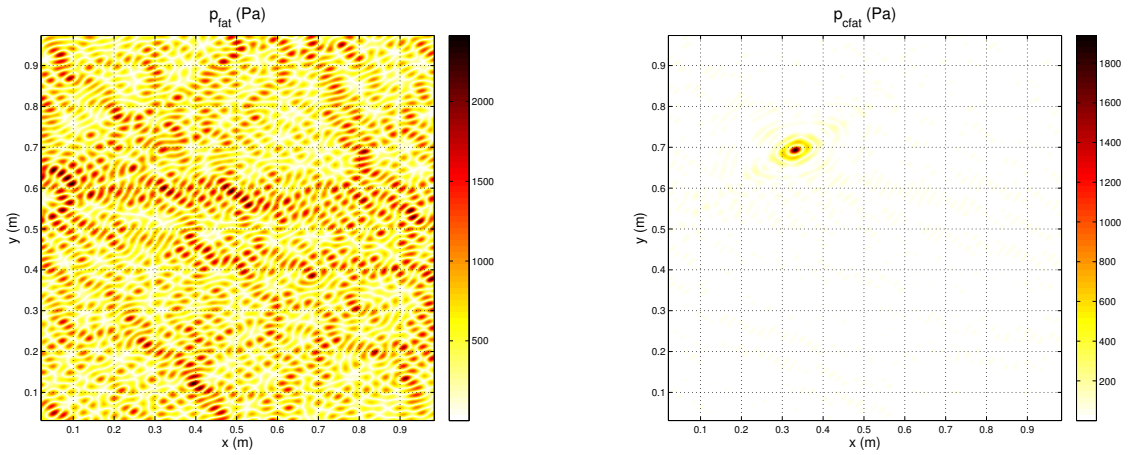

Figure 8: Pressure field estimated with FAT and CFAT_{num} (50 equations) on the laminated structure with $n_x = n_y = 3$.

The pressure fields estimated by FAT doesn't allow us to clearly identify the source. On the contrary, CFAT attenuates the level of pressure in the non loaded area (as it should be in reality) which reveals the localisation of the source.

Other experimentations were done with the laminated plate in order to show the influence of the number of points per wavelength on CFAT. For that, we have chosen 3 values of (n_x, n_y) (see Figure 9). Noise was added to the displacement field in order to get closer to the experimental conditions with a signal-to-noise ratio approximately equal to 14 dB for all configurations.

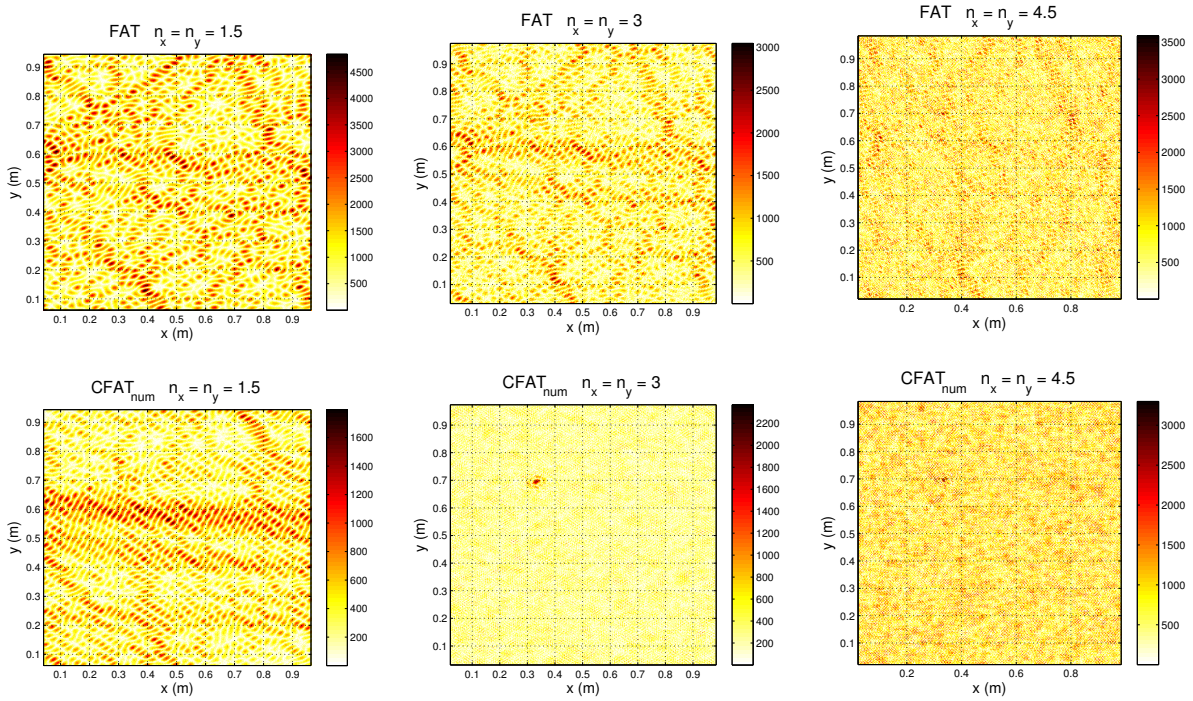

Figure 9: Evolution of the pressure field (Pa) estimated with FAT and CFAT on the laminated structure in function of n_x and n_y.

When the number of points per wavelength is under the condition quoted in Eq. (8), the estimation of the pressure field is totally wrong. With an optimal number of points, the source is well located even with noise. With a high number of points, the level of noise is amplified and exceed the level of the source. Only noise is dominating the pressure field and the identification of the

source is then impossible with the both methods. Moreover, in this last case, correction is useless because the finite difference scheme can clearly estimate the partial derivatives. So, the correction factors tend to 1 and there is no difference between FAT and CFAT estimation, as we can see in the right part of Figure 9. That's why, in experimental condition with noise, an optimal value of the number of point proves the usefulness of CFAT method.

A quantification of the force has been realised from FAT and CFAT estimations on the laminated plate in function of the frequency. The force at the excitation has been calculated by integrating the pressure field over 15 x 15 points ($12,25$ cm^2) around the maximum of pressure identified with CFAT in Figure 8. For each methods, Figure 10 compares this force with the mean square residual force in the rest of the plate:

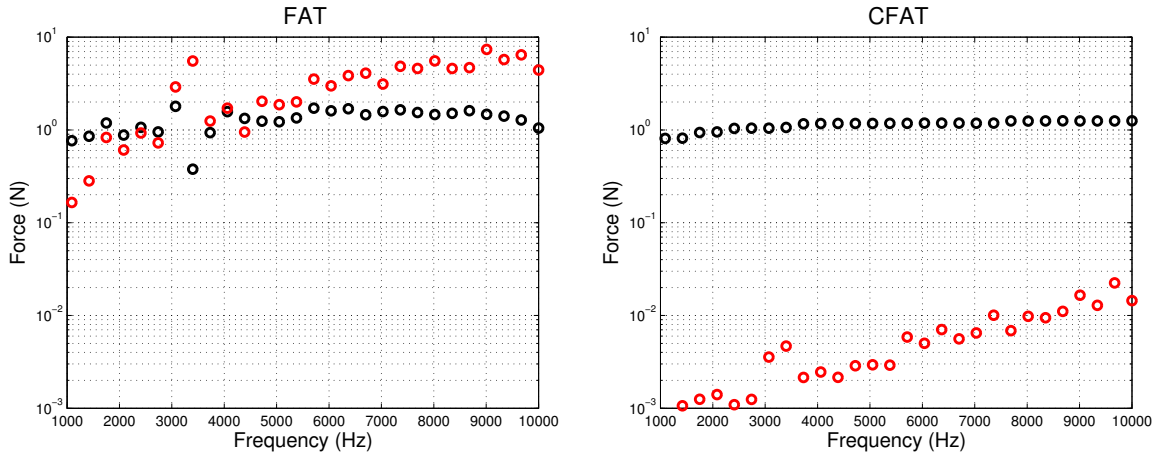

Figure 10: Comparison between the quantification of the force at the excitation point (black circle) and the mean square residual force in the non loaded area (red circle) from FAT and CFAT methods in the laminated case.

The observations made previously from Figure 8 leads to the same conclusions for the quantification of the force. For both methods, the estimation of the force at the excitation point is close to the imposed force on Nastran (1 N). However, contrarily to the CFAT case, the force identified by FAT is biased by the high level of pressure in the non loaded area.

4 CONCLUSION

In this paper, the extension of CFAT (Corrected Force Analysis Technique) method has been developed to identify sources applied on laminated (composite) structures. The equation of motion of this type of structures involves to use a more complex scheme with an estimation of 5 partial derivatives. This estimation requires to apply 5 correction factors on the scheme which can be identified analytically or numerically. The numerical aspect shows a better distribution of the attenuation of the singularity created by the finite difference scheme and is better to implement. Numerical validations on noised displacement field reveals that the adaptation of the scheme and the number of points per wavelength at each frequency is essential in the process of the method to avoid bias error. By respecting this condition, CFAT gives best results with a reduction of the level of pressure estimated in the non loaded area.

Recent papers present CFAT as a characterization method for isotropic or orthotropic materials. Finally, this adaptation could also be developed for the characterization of composite structures.

REFERENCES

[1] K.S. Stevens. Force identification problems: an overview. *Proceedings of SEM Spring Conference on Experimental Mechanics*, pages 838–844, 1987.

[2] C. Pézerat and J.-L. and Guyader. Two inverse methods for localization of external sources exciting a beam. *Acta Acustica*, 3:1–10, 1995.

[3] C. Pézerat and J.-L. Guyader. Force analysis technique : reconstruction of force distribution on plates. *Acustica United with Acta Acustica*, 86:322–332, 2000.

[4] M.S. Djamaa, N. Ouella, C. Pézerat, and J.-L. Guyader. Reconstruction of a distributed force applied on a thin cylindrical shell by an inverse method and spatial filtering. *Journal of Sound and Vibration*, 301:560–575, 2007.

[5] Q. Leclère, F. Ablitzer, and C. Pézerat. Identification of loads of thin structures with the corrected force analysis technique: An alternative to spatial filtering regularization. *Proceedings of ISMA 2014*, 2014.

[6] Q. Leclère and C. Pézerat. Vibration source identification using corrected finite difference schemes. *Journal of Sound and Vibration*, 331(6):1366–1377, 2012.

[7] F. Ablitzer, C. Pzerat, J.-M. Gnevaux, and J. Bgu. Identification of stiffness and damping properties of plates by using the local equation of motion. *Journal of Sound and Vibration*, 333(9):2454 – 2468, 2014.

[8] Q. Leclere, F. Ablitzer, and C. Pézerat. Practical implementation of the Corrected Force Analysis Technique to identify the structural parameter and load distributions. *Journal of Sound and Vibration*, 351:106–118, 2015.

[9] F. Ablitzer, C. Pézerat, B. Lascoup, and J. Brocail. Identification of the flexural stiffness parameters of an orthotropic plate from the local dynamic equilibrium without a priori knowledge of the principal directions. *Journal of Sound and Vibration*, 404:31 – 46, 2017.

[10] F. Marchetti, K. Ege, and Q. Leclère. Modèle monocouche équivalent de plaque multicouche orthotrope. In *Congrès Français de Mécanique, CFM 2017*, Lille, France, August 2017.